ELSEVIER

Marine and Petroleum Geology 16 (1999) 97–110

Marine and Petroleum Geology

Combined use of Confocal Laser Scanning Microscopy and PVT simulation for estimating the composition and physical properties of petroleum in fluid inclusions

A.C. Aplin[a,*], G. Macleod[a,1], S.R. Larter[a], K.S. Pedersen[b], H. Sorensen[b], T. Booth[c]

[a] *Fossil Fuels and Environmental Geochemistry Postgraduate Institute: NRG, Drummond Building, University of Newcastle, Newcastle upon Tyne, NE1 7RU, UK*

[b] *Calsep A/S, Gl. Lundtoftevej 7, DK-2800, Lyngby, Denmark*

[c] *Biomedical Electron Microscopy Unit, The Medical School, University of Newcastle, Newcastle upon Tyne, NE1 7RU, UK*

Received 12 June 1998; revised 12 November 1998; accepted 26 November 1998

Abstract

We present a method to determine the composition and PVT properties of petroleum in individual petroleum fluid inclusions. Confocal Laser Scanning Microscopy is used to generate three dimensional images of single petroleum inclusions. Because liquid petroleum fluoresces under the laser, the images readily distinguish the liquid and vapour within the inclusion and can be used to determine the inclusion's volumetric liquid:vapour ratio. Using PVT modelling software, the liquid:vapour ratio is used along with the homogenisation temperature to determine the bulk composition, phase envelope, isochore and a range of physical properties of the included petroleum. This is done using an iterative series of PVT calculations which match two parameters: (1) the molar volume of the petroleum at room and homogenisation temperatures; (2) the liquid:vapour ratio of the inclusion at room temperature. Key uncertainties in the method are explored, including the accuracy with which the liquid:vapour ratio can be determined; the composition of the titrant gas used in the iterative procedure; and the composition of the petroleum chosen to model the physical properties of the included petroleum. Data from coeval inclusions suggest that the saturation pressure, Gas–Oil Ratio, viscosity, molar volume, density and surface tension of included petroleum are determined with a *precision* of a few percent. Confirmation of the *accuracy* of the method awaits tests using inclusions grown in the laboratory under carefully controlled PVTX conditions. However, it is likely that the physical properties of included petroleums are more accurately modelled by fluids which are genetically related to them. If proven to be accurate, the method will provide a routine method for determining palaeopressure in petroleum systems. Finally, we present data from a Central North Sea example which are geologically realistic and which for the first time record the evolution of fluid pressure and petroleum composition in a petroleum reservoir. © 1999 Elsevier Science Ltd. All rights reserved.

Keywords: Confocal microscopy; PVT simulation; fluid inclusions; palaeobarometry

1. Introduction

Tiny capsules of petroleum are commonly trapped as fluid inclusions within petroleum reservoir units and carrier beds in sedimentary basins (McLimans & Horsfield, 1984; Narr & Burruss, 1984; McLimans, 1987; Jensenius & Burruss, 1990; Bodnar, 1990; Earnshaw, Hogg, Oxtoby & Cawley, 1993; Karlsen, Nedkvitne, Larter, & Bjørlykke, 1993; Swarbrick, 1994; Larese & Hall, 1996). The inclusions can yield two types of information

1. The source and maturity of the petroleum, if the petroleum can be extracted and analysed (Karlsen et al., 1993; Jones et al., 1996, Lisk, George, Summons, Quezoda, & O'Brien, 1996; Isaksen, Pottorf, & Jenssen, 1998).
2. The pressure and temperature at which the inclusion was trapped (see Roedder (1984) and Goldstein & Reynolds (1994) for extensive reviews).

The minimum *temperature* of trapping is determined routinely as the temperature at which the fluid inclusion homogenises into a single phase upon heating in the laboratory. In contrast, the minimum trapping pressure cannot be measured directly and can only be assessed if the P–T phase diagram of the petroleum can be defined. This requires that the composition of the included petroleum be known.

[1] Present address: Shell Exploration and Production Technology Co., Bellaire Technology Center, 3737 Bellaire Boulevard, P.O. Box 481, Houston, TX 77025, USA

* Corresponding author. Tel.: +44-191-222-2605; fax: +44-191-222-5431; e-mail: nrg@ncl.ac.uk

0264-8172/99/$ - see front matter © 1999 Elsevier Science Ltd. All rights reserved.
PII: S0264-8172(98)00079-8

A variety of direct and indirect methods has been used to estimate the composition of petroleum inclusions. Direct methods involve crushing inclusions and analysing their contents using gas chromatography or gas chromatography-mass spectrometry (Burruss, 1987, 1992; Karlsen et al., 1993; Macleod, Larter, Aplin, & Petch, 1994; Macleod, Larter, Aplin, & Bigge, 1995; Bigge, Petch, Macleod, Larter, & Aplin, 1995; Jones et al., 1996). There are three difficulties with this approach. Firstly, contamination of included petroleum with reservoired petroleum is difficult to estimate. Secondly, many inclusions must be crushed in order to obtain an analysis, resulting in an average petroleum composition with components from both petroleum and aqueous inclusions. Thirdly, the quality of the chromatogram depends on the abundance of inclusions (Macleod et al., 1994, 1995; Bigge et al., 1995). Although rare samples with high densities of inclusions yield excellent chromatograms, our own experience suggests that it is more common to observe chromatograms which appear to be much richer in gas than is likely based on their geological setting and their petrographic appearance.The composition of petroleum inclusions can also be assessed using a variety of micro-spectroscopic techniques such as UV-epi-fluoresecence (Bodnar, 1990, Guilhaumou, Szydlowskii, & Pradier, 1990), Infra Red Spectroscopy (Guilhaumou et al., 1990), FT-IR (Pironon & Barrés, 1990, 1992) and UV-fluorescence excitation emission spectroscopy (Kihle, 1996). Although these techniques have the benefit of analysing single inclusions, they do not give a sufficiently detailed composition to allow accurate PVT modelling of the included petroleum.

In this paper we report a completely new approach to the determination of the composition of petroleum in single inclusions and to the derivation of its PVT properties. We describe how Confocal Laser Scanning Microscopy (CLSM) can be used to determine the volumetric liquid:vapour volume ratio of petroleum inclusions and how this information can be used in association with commercially available simulators of petroleum phase behaviour to determine P–T phase diagrams, isochores, viscosity, and Gas–Oil Ratio ($GOR = C_1–C_5/C_{6+}$ at STP conditions of 15°C and 1 bar) of the petroleum trapped within individual inclusions.

2. PVT properties of petroleum fluid inclusions

Fig. 1 shows a P–T phase diagram for a multicomponent petroleum fluid. The phase envelope comprises a bubble point curve and a dew point curve which meet at the fluid's critical point. The phase envelope separates regions in P–T space in which the fluid exists as a single phase (gas or liquid) or as two phases (liquid plus gas). Imagine that a single phase, liquid petroleum fluid inclusion had formed at point A in Fig. 1 and consider what happens to that inclusion when it is brought to room conditions. Because the volume of the inclusion is fixed, the density and molar volume of the inclusion contents also remain fixed as the P–T conditions change. Upon cooling, the P–T conditions within the inclusion are thus constrained to fall on an isochore (line of constant density and also molar volume (A–B on Fig. 1)). Point B is the bubble point of the petroleum, the point at which the first vapour bubble is exsolved from the fluid. Continued cooling will result in continued exsolution of vapour and an increase in the liquid:vapour ratio of the inclusion. At room conditions (point C on Fig. 1), the fluid inclusion is a two phase liquid plus vapour system; its temperature is that of the room but its pressure is higher than atmospheric. The petroleum in the inclusion can be homogenised back into a single phase by reheating it in the laboratory. The homogenisation temperature, which can be measured to ± 0.1°C, is the temperature at which the P–T conditions in the heated inclusion intersect the bubble point or dew point curves of the included petroleum (Fig. 1). This point is also known as the saturation temperature and pressure of the petroleum. An included oil will homogenise to a liquid at the homogenisation temperature whereas a gas or retrograde gas (gas condensate) will homogenise to a critical or single phase gaseous state. The homogenisation temperature and pressure are thus the minimum trapping temperature and pressure of the inclusion, the true trapping temperature and pressure lying somewhere along the pet-

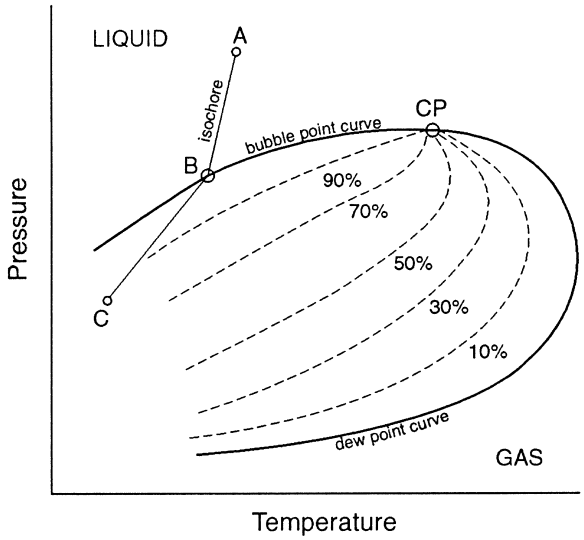

Fig. 1. PT phase diagram of a multicomponent petroleum. CP is the critical point of the fluid and the curves to the left and right of the critical point are the bubble point and dew point curves. As it is taken to surface conditions (C), the path taken by a petroleum trapped as an inclusion at point A is from A to B (bubble point or saturation temperature and pressure) along the fluid's isochore, and then through the two phase region to C. Dashed lines in the two phase region are lines of equal percent liquid and vapour.

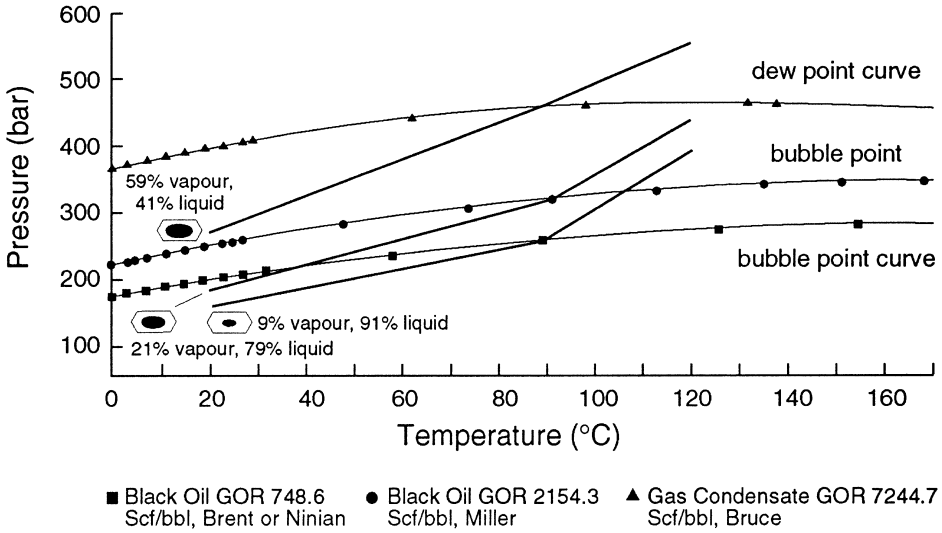

Fig. 2. Parts of the phase envelopes of three compositionally distinct petroleums (two oils and one gas-condensate) calculated using PVTSIM. Also shown are the calculated isochores of hypothetical petroleum fluid inclusions trapped with the appropriate composition and with homogenisation temperatures of 90°C, along with the predicted volume % vapour and liquid of each inclusion at room temperature.

roleum's isochore in the single phase region of the P–T diagram.

Parts of the phase envelopes of two oils and one gas condensate are shown in Fig. 2. These envelopes and isochores were calculated from the mole percent composition of the petroleums (data from field operators) using the PVT simulation package PVTSIM (Pedersen, Fredenslund, & Thomassen, 1989). PVTSIM uses the modified Soave–Redlich–Kwong equation of state and calculates standard parameters such as fluid compressibility, density, saturation pressure and temperature from a compositional analysis, also constructing a phase envelope. It also determines the fluid properties of the petroleum at a range of P–T conditions. Although the minimum compositional input requirements for PVTSIM are mole percent of C_1–C_6 alkanes and isoalkanes, inorganic gases plus a single value for C_{7+}, more detailed analyses will yield better results; a C_1–C_{19} plus C_{20+} analysis is thus desirable (Pedersen et al., 1989). Many other PVT packages are available; they use different equations of state but appear to give similar results away from temperatures and pressures near to the critical point (Pedersen et al., 1989; Danesh, Xu, & Todd, 1991). We have used PVTSIM and VTFLINC, a sister program written specifically for fluid inclusion applications, in all the work presented in this paper.The PVT simulation software can be used to calculate the internal pressure and liquid:vapour ratio of included petroleum at any temperature at which an inclusion might be viewed under the microscope. To illustrate this, let us use the three hypothetical inclusions with compositions defining the phase envelopes in Fig. 2, and assume that they all homogenise at 90°C. Using the mole % composition of the petroleum as input, the PVT software calculates the molar volume, saturation pressure and density of the petroleum at the homogenisation temperature (90°C). It also calculates the saturation pressure at room temperature. Since the included petroleum actually comprises liquid plus vapour at room temperature, the saturation pressure at room temperature is greater than the true internal pressure of the inclusion and the molar volume at saturation pressure is correspondingly lower than the true molar volume of the inclusion's contents. The true internal pressure of the inclusion at room temperature can be calculated by iteratively adjusting the pressure and recalculating the molar volume of the overall contents until they agree with the molar volume calculated for the contents at the saturation temperature (90°C) and pressure. An isochore can then be constructed tying the pressures at room and saturation temperatures. Similar calculations allow one to construct an isochore in the single phase region of the phase diagram. A analogous procedure using total petroleum densities can be employed, but is less accurate in the two phase region.

Having defined the internal pressure of the inclusion at room temperature, the PVT software can then be used to calculate the volumetric liquid : vapour ratio of the petroleum at that pressure. Fig. 2 shows that the volumetric liquid:vapour ratios of the three petroleums used in this example are radically different: the more gas-rich petroleums have lower liquid:vapour ratios. Reheating the inclusion under the microscope moves the included petroleum along the isochore in P–T space to the phase envelope relevant to its composition, at which point it will homogenise into the appropriate single phase: liquid for the two oils and gas for the gas-condensate.

The analysis described above shows that PVT simulation software can be used in conjunction with the homogenisation temperatures of included petroleums of known composition to determine

1. Liquid:vapour ratios and internal pressures at room temperature.
2. Saturation pressures at both homogenisation (bubble or dew point) and room temperatures.
3. Isochores. In this paper we invert the analysis presented above. Here, we use the measured homogenisation temperature of a petroleum inclusion along with its liquid:volume ratio at room temperature to determine the petroleum's saturation pressure, isochore and phase envelope, plus the internal pressure of the fluid inclusion at laboratory conditions.

Three pieces of information are required

1. The inclusion's homogenisation temperature, which can be determined microthermometrically.
2. The inclusion's volumetric liquid:vapour ratio at room conditions. This, as we describe in this paper, can be determined by CLSM.
3. The composition of the included petroleum, or at least a composition which is sufficiently detailed to enable the accurate prediction of its physical behaviour. Since there is no way of extracting and analysing petroleum from a single inclusion, this is the most difficult task facing us. One methodology for estimating the composition of included petroleum, based on the iteration of PVTX properties within a petroleum PVT simulator, is presented in a later section of the paper.

3. Confocal Laser Scanning Microscopy

Over the last decade CLSM has gained wide acceptance as a method for generating three-dimensional images of thick specimens. The principles and applications of CLSM are described in detail by Sheppard & Shotton (1997). Briefly, light from a laser passes through a pinhole aperture and is focused by an objective lens to a sub-micron size spot on the specimen. Reflected or secondary light (e.g. fluorescence) is collected by the objective lens and partially refracted towards a second pinhole aperture in front of the detector. In this way the only light arriving at the detector is that deriving from the focal plane of the microscope; out of focus light is rejected. Since the confocal microscope delivers a point image, a two-dimensional x–y image slice of the specimen is built up by rapidly scanning the specimen using galvanometer-driven mirrors. A pseudo three-dimensional image is obtained by taking a series of confocal images at successive planes down through the specimen (a 'z' series). Each point image is digitised and stored in a computer, allowing image processing and construction of in-focus, pseudo-3D images.

In our work we have exploited the ability of the CLSM to obtain pseudo three-dimensional images to determine the volumetric liquid:vapour ratios of petroleum inclusions (Macleod, Larter, Aplin, Pedersen, & Booth, 1996). This cannot be done by conventional microscopy because the two-dimensional image cannot be converted to volumetric data without erroneous assumptions about the shape of the inclusion. Doubly polished wafers of reservoir rocks, previously used for microthermometry, were studied on the CLSM under oil immersion with a $\times 60$ magnification lens. We used a Nikon Optiphot II microscope with an attached Biorad MRC 600 confocal laser unit. The laser delivers a power of around 1.5 mW to the objective lens and a single frame in the z series is accumulated in 1 s. Under these conditions heating of the inclusion is minimal. The horizontal (x–y) resolution of the microscope is around 0.2 μm and the vertical resolution of 0.1 μm is determined by the precision with which the stepper motor drives the microscope stage. The CLSM is controlled by a microcomputer running the commercial COMOS software (version 6.05); this software was also used for the analysis of the resulting images. The Kr–Ar laser produces excitation lines at 488, 568 and 647 nm. In this study the petroleum inclusions were excited at 488 nm, with K1 and K2 filters. The petroleum within the inclusions fluoresces brightly when excited at this wavelength, emitting strongly in regions around 520 nm and allowing the differentiation of liquid and vapour parts of the inclusion (Fig. 3).

Having determined the homogenisation temperature of the inclusion (we used a modified USGS heating-freezing stage), the following procedure is used to determine the volume percent of vapour and liquid. The computer controlled stage is used to locate the top and bottom of the inclusion by visual observation. Scans are then made at approximately 1 μm steps through the inclusion. The separate two-dimensional images through the inclusion can then be processed by image analysis software by assigning one colour threshold/greyscale to the liquid part of the inclusion and another to the vapour bubble. The volume of vapour and liquid in each image slice can then be determined using, for example, the equation describing the volume of an irregular cylinder. Summation of the slices gives the total volume fraction of vapour and liquid inside the inclusion.

Fig. 3 shows some of the z-series images taken through an irregular, 10 μm petroleum fluid inclusion hosted in diagenetic quartz from the North Sea's Alwyn Field. Both the top and bottom of the inclusion are full of liquid, with a vapour bubble located in the core of the inclusion. Table 1 gives the areas and volumes of liquid petroleum and vapour for this inclusion. In this case, the estimated liquid:vapour ratio using white light on a conventional stage was 80% liquid : 20% vapour, compared to 90.7% liquid : 9.3% vapour determined using the CLSM. Differences of this magnitude in the liquid: vapour ratio will alter enormously the assessment of the PVTX properties of the petroleum.The accuracy with which the internal structure of the inclusion can be imaged is limited by several factors. Firstly, the microscope's inherent limitations include the spot size of the

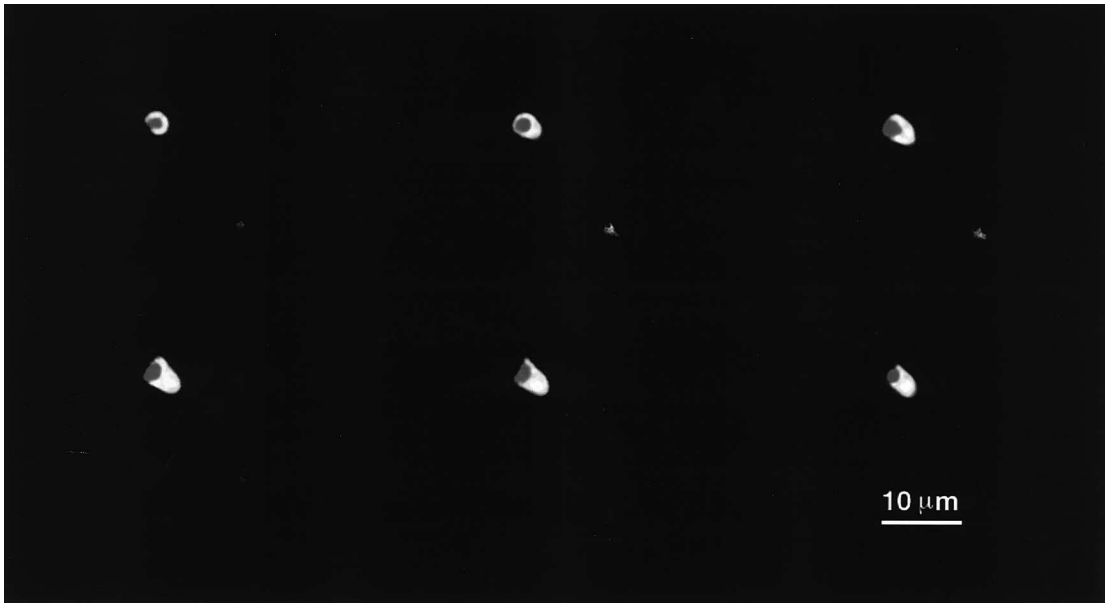

Fig. 3. Six of the twelve images of the z series taken with the Confocal Laser Scanning Microscope through an 11 μm deep inclusion hosted in diagenetic quartz from the North Sea's Alwyn Field. Passing down through the inclusion the vapour bubble (grey) appears and disappears, and the internal shape of the inclusion changes.

Table 1
Calculated areas of liquid and vapour in images taken with a Confocal Laser Scanning Microscope as a z series through a petroleum fluid inclusion. The inclusion is primary, 10 μm in diameter and is hosted within diagenetic quartz from the North Sea's Alwyn Field. The inclusion has a homogenisation temperature of 92.2 °C[a]

Depth μm	Total area μm^2	Area of vapour μm^2	Area of liquid μm^2
0	11.0	0.0	11.0
1	13.1	0.4	12.6
2	15.7	0.3	15.5
3	18.9	3.1	15.8
4	21.2	4.4	16.8
5	24.2	5.6	18.7
6	23.9	3.9	20.0
7	24.8	1.5	23.3
8	22.0	0.0	22.0
9	17.8	0.0	17.8
10	9.1	0.0	9.1
11	3.3	0.0	3.3
12	0.0	0.0	0.0

[a] Inclusion volumes: total volume = 205.2 μm^3; total vapour volume = 19.1 μm^3; total liquid volume = 186.1 μm^3; % liquid = 90.7; % vapour = 9.3.

laser (0.2 μm) and its vertical resolution (0.1 μm). Secondly, flaring at the boundary of brightly fluorescing liquid and non-fluorescing vapour and mineral can cause uncertainty in the accurate definition of the phase boundaries. Thirdly, the vapour bubbles are imaged as ellipses, elongated along the z axis. The true shape of the vapour bubble may approximate a sphere but will also depend on the surface topography of the inclusion and the position of the vapour bubble relative to the inclusion surface. We are not certain why the vapour bubble is imaged as an ellipse but believe that it is partly due to optical stretching caused by refractive index differences between the immersion medium and host mineral. For our purposes, this is only a problem if the alteration of the image leads to a change in the relative amounts of liquid and vapour and we have assumed that optical stretching occurs homogeneously in the z direction. Although this important uncertainty requires resolution, the consistency of the data generated by the technique (see later) suggests that the problem is not severe.

4. PVTX of included petroleum

Along with the liquid:vapour ratio of the included petroleum and its homogenisation temperature, the third piece of information that we need to calculate the phase envelope and isochore of the petroleum is its composition, or at least a composition which accurately mimics the petroleum's physical properties. Since an accurate composition is difficult to determine directly, the composition must be estimated indirectly. This is done using an iterative series of PVT calculations which match two parameters: (1) the molar volume of the petroleum at room and homogenisation temperature; (2) the liquid:vapour ratio of the inclusion at room temperature. The calculations can be performed with commercially available PVT simulation software and are outlined below:

1. Choose the composition of an initial petroleum with which to start the simulation, for example from a nearby reservoir.
2. Using a PVT simulator, calculate the saturation pressure of the chosen petroleum at the saturation temperature (homogenisation temperature) of the inclusion.
3. Perform a 'flash' or phase fraction-composition calculation at homogenisation temperature and saturation pressure, noting the total molar volume of the petroleum.
4. Calculate the saturation pressure of the initial petroleum at room temperature. Since the included petroleum exists as two phases, the saturation pressure is the maximum possible pressure within the inclusion.
5. Perform a series of 'flash' or vapour-liquid equilibrium calculations at room temperature and at a series of pressures below the calculated saturation pressure. These calculations determine the volume and composition of liquid and gas phases. Note the molar volume of the petroleum in each case. When the molar volume of the mixture at room temperature matches the molar volume calculated at the homogenisation temperature, the two points are linked in P–T space; that is, they lie on the same isochore. The same calculation can be performed using the density of components but is less accurate since the densities of individual phases in the two phase region are more poorly constrained.
6. Calculate the liquid:vapour ratio of the initially chosen petroleum at room temperature and the calculated internal pressure of the included petroleum. If the calculated volume % of vapour and liquid at that temperature and pressure match that measured using the CLSM, then the composition of the chosen petroleum is an accurate physical representation of the petroleum within the inclusion.
7. If the calculated volume % of vapour and liquid in the inclusion do *not* match the measured values, titrate gas into or out of the initial petroleum and repeat the entire calculation. As shown in the next section, the choice of gas composition is critical to the success of the iterative procedure.
8. Repeat steps 2–7 until the calculated volume % vapour and liquid match the measured values. The composition of the petroleum is now very close to that of the included petroleum, or is at least an 'effective composition' because it accurately mimics its PVT properties. The final composition can now be used to construct phase envelopes and isochores for the included petroleum.

5. Uncertainties

Until we are able to grow petroleum inclusions in the laboratory under known PVTX conditions, it is impossible to know that calculated physical properties of the included petroleums are *accurate*. In this section we describe the results of a series of tests we have conducted to determine the *precision* of the methodology. Four areas of uncertainty are examined: (1) the microscopic determination of the liquid:vapour ratio; (2) the composition of the gas titrated into or out of the model petroleum; (3) the composition of the initial petroleum chosen to model the physical properties of the included petroleum and (4) the difference between the saturation and true trapping pressure.

5.1. Liquid:vapour volume ratio

In this test we assume that a petroleum of known composition has been trapped in a fluid inclusion which has a homogenisation temperature of 90°C. In order to simulate uncertainty in the determination of the inclusion's liquid:vapour ratio, we have allowed the measured volume % vapour of the inclusion to range from 9 to 11%. Starting with a petroleum which is compositionally different to that of the included petroleum, we have then used the PVT simulation software to determine the saturation pressure and GOR of inclusions with 9, 10 and 11% vapour. The results (Table 2) show that an increase in volume percent vapour by 1% increases

Table 2
Effect of % vapour on calculated saturation pressure and gas–oil ratio of included petroleum. Identical model petroleums and modelling strategies were used in all cases

Volume vapour (%)	Pressure (bar)	GOR (Sm^3/Sm^3)
9	238.25	127.56
10	254.36	147.53
11	267.78	167.46

the calculated saturation pressure by about 20 bar and the calculated GOR by about 20 Sm^3/Sm^3.

5.2. Composition of titrant gas

The composition of the gas titrated into or out of the initially chosen petroleum exerts an important influence on the calculated PVT properties of included petroleum. We have tested four methods for estimating the composition of the gas used to titrate into the model petroleum during the iterative procedure. Method (1) first calculates the saturation pressure at the observed homogenisation temperature of the chosen petroleum and then calculates the composition of the first gas formed at a pressure just below the bubble point. In Method (2), the gas composition is the equilibrium gas composition derived from a flash of the chosen petroleum to STP. In Method (3), the gas composition is taken as the equilibrium gas from a flash of the initially chosen petroleum composition at 1 atmosphere pressure and the homogenisation temperature. In Method (4), the gas composition is the equilibrium gas derived from a flash of the chosen petroleum at 1 atmosphere pressure and a temperature 50°C higher than the homogenisation temperature.

We have tested each method by conducting two very different test simulations. In the first case we have taken a petroleum of known composition which has been trapped in a fluid inclusion which homogenises at 90°C. Table 3 lists the calculated (PVTSIM) properties of this petroleum at 15°C and 1 atmosphere, plus its saturation pressure at 90°C. The composition of the petroleum chosen to test the different calculation methodologies is very different to that of the included petroleum, having a GOR of 133 Sm^3/Sm^3 compared to 384 Sm^3/Sm^3 for the included petroleum. Table 3 lists the physical properties of the petroleums which have been calculated iteratively by titrating the four possible gas compositions into the chosen petroleum.

The second test is similar to the first but in this case the GOR of the fictitious, included petroleum is much lower than that of the petroleum chosen to calculate the physical properties of the included petroleum (133 vs 370 Sm^3/Sm^3). Table 4 lists the calculated properties of this petroleum, plus the results of the iterative PVT calculations.

In both tests, the closest agreement between the actual and calculated physical properties of the included petroleum was obtained using Method (4). Since the iterative procedure forces the volume of gas and liquid to the measured values, these numbers provide no test of the procedure. However, the results from Method (4) agree well the fluid's true molar volume (1% different), density (2–3%), GOR at STP (0.5–5%) and saturation pressure at 90°C (6–10%). None of the other methods give such good agreement over the full range of parameters. Method (4) generates and titrates a more realistically wet (higher ratio of C_1–C_4/C_1) gas into or out of the chosen petroleum. It appears to give reasonably accurate results even when the initially chosen petroleum is compositionally very different to that in the inclusion. This has some geological justification in that included petroleums frequently differ in maturity from reservoir petroleums over a maturity range where gas wetness does not usually change significantly.

5.3. Composition of initial, model petroleum

Table 5 gives the compositional breakdown of five petroleums and two recombined petroleums which we have used to test the influence that the composition of the initially selected petroleum exerts on the calculated properties of included petroleums. In order to provide extreme tests for the computational procedures, we have purposefully selected petroleums with extremely diverse compositions, generated from different source rocks. These include both North Sea and North American petroleums.

Table 3
Calculated (using PVTSIM) properties of a petroleum in a hypothetical fluid inclusion with a homogenisation temperature of 90°C. 'Correct values' are those calculated by PVTSIM at 15°C and 1 atmosphere, plus the saturation pressure at 90°C. Other columns give the properties of the included petroleum calculated iteratively by titrating gas compositions derived by flashing a model petroleum at a range of pressure and temperature conditions (see text). The model petroleum has a GOR of 133 Sm^3/Sm^3

Parameter	Correct value	Method 1	Method 2	Method 3	Method 4
Sat^n P at 90°C (bar)	321	501	456	403	344
GOR (m^3/m^3)	384	339	352	363	364
Density (g/cm^3)	0.5766	0.6339	0.6338	0.6143	0.5915
Molar volume at 15°C (cm^3)	103.1	102.5	103.3	102.3	101.9
Volume gas at 15°C (%)	21.3	21.3	21.3	21.3	21.3
Volume liquid at 15°C (%)	78.7	78.7	78.7	78.7	78.7

Table 4
Calculated (using PVTSIM) properties of a petroleum in a hypothetical fluid inclusion with a homogenisation temperature of 90°C. 'Correct values' are those calculated by PVTSIM at 15°C and 1 atmosphere, plus the saturation pressure at 90°C. Other columns give the properties of the included petroleum calculated iteratively by titrating gas compositions derived by flashing a model petroleum at a range of pressure and temperature conditions (see text). The model petroleum has a GOR of 370 Sm^3/Sm^3

Parameter	Correct value	Method 1	Method 2	Method 3	Method 4
Sat^n P at 90°C (bar)	260	146	164	204	238
GOR (m^3/m^3)	133	121	109	123	134
Density (g/cm^3)	0.7264	0.6912	0.6967	0.7059	0.7134
Molar volume at 15°C (cm^3)	148.6	148.7	149.3	149.8	150.1
Volume gas at 15°C (%)	9.5	9.5	9.5	9.5	9.5
Volume liquid at 15°C (%)	90.5	90.5	90.5	90.5	90.5

Table 5
Composition of petroleums used to model the PVTX properties of four coeval, secondary, petroleum inclusions in quartz from a North Sea reservoir

	N. Sea 1 mole %	N. Sea 2 mole %	N. Sea 3 mole %	N. Sea 4 mole %	N. Sea 5 mole %	N. Sea 6 mole %	N. Am 1 mole %	N. Am 2 mole %
Component								
N_2	0.534	1.26	1.02	0.09	0.328	0.79	0.42	
CO_2	2.442	1.14	3.96	1.91	1.472	5.76	0.28	0.84
C_1	54.916	48.7	54.7	44.21	67.554	59.84	62.06	26.57
C_2	9.016	10.17	11.36	6.48	6.782	12.61	9.5	10.74
C_3	6.037	6.6	6.41	4.34	3.093	5	6.19	9.27
iC_4	0.739	0.92	0.93	0.53	0.426	0.82	1.28	0.52
nC_4	2.472	3.19	2.2	1.91	1.206	1.73	2.54	6.3
iC_5	0.818	0.79	0.77	0.78	0.352	0.67	0.98	1.26
nC_5	1.326	1.38	1.12	1.59	0.667	0.77	1.39	3.92
C_6	2.208	1.96	1.59	4.14	1.199	1.05	2.26	1.76
$C_{7(+)}$	3.464	23.89[e]	15.94[f]	34.02[h]	2.834	10.96[g]	13.6[a]	38.82[b]
C_8	2.939				2.767			
C_9	1.483				2.4			
C_{10}	0.972				8.919[d]			
C_{11}	1.198							
C_{12}	0.962							
C_{13}	0.925							
C_{14}	0.793							
C_{15}	0.675							
C_{16}	0.585							
C_{17}	0.586							
C_{18}	0.51							
C_{19}	0.407							
C_{20}	3.993[c]							

[a] Molecular weight = 180; density = 0.818 g/cc.
[b] Molecular weight = 207; density = 0.848 g/cc.
[c] Molecular weight = 440; density = 0.904 g/cc.
[d] Molecular weight = 224.3; density = 0.826 g/cc.
[e] Molecular weight = 244; density = 0.845 g/cc.
[f] Molecular weight = 229.9; density = 0.828 g/cc.
[g] Molecular weight = 195; density = 0.815 g/cc.
[h] Molecular weight = 233; density = 0.871 g/cc.

The tests were carried out on four secondary inclusions within quartz from a Central North Sea reservoir currently at its maximum temperature (120°C). The inclusions appear to have formed coevally and have a range of homogenisation temperatures between 68.3 and 69.9°C. None of the chosen petroleums come from the

same field as the inclusions. Two (North Sea 2 and 3) are from fields within 20 km of the inclusions and were generated from the Kimmeridge Clay Formation, the regional source rock. North Sea 1 was also generated from the Kimmeridge Clay but is reservoired 500 km to the north of the area from which the inclusions come. North Sea 4 was generated from the Kimmeridge Clay and is reservoired in the Central Graben around 100 km from the inclusions. North Sea 6 is a recombined petroleum from the same area as North Sea 3. The fluid in this reservoir is a gas condensate (%CH_4 = 64.5; %C_1–C_4 = 82.4). We have found that the PVT simulation program is unable to calculate the properties of low GOR oils from such gas-rich starting compositions. To overcome this problem, the initial reservoired petroleum was flashed using the PVT simulator at standard temperature and pressure. The liquid and gas phases were then recombined in new proportions to give a less gas-rich, hypothetical starting fluid with a GOR of 534 Sm^3/Sm^3 (3000 scf/bbl) and a density of 0.8 gcm^{-3}. A similar procedure was adopted for North Sea 5, which is a gas condensate from the same field as North Sea 1. In the reservoir, this fluid contains 78.6% CH_4 and 91.7% C_1–C_4.

The North American petroleums were chosen because their compositions are radically different from those of the North Sea petroleums (Table 5). The North American black oil is particularly unusual in that it is very depleted in methane and has a high proportion of C_{7+} compounds with a mean molecular weight much lower than those of the North Sea fluids. One would therefore anticipate that the PVT properties of these North American oils will be very different to those of the North Sea petroleums.

In all these tests the composition of the titrant gas was derived using Method 4 (see above). The results are shown in Table 6. By starting with the three North Sea oils, all of which have a much higher GOR and methane contents than the included petroleums, the calculated physical properties of the petroleum in a single inclusion are almost identical: a range of 15 bar for the saturation pressure and a range of 6 Sm^3/Sm^3 for the GOR. If the results from the recombined petroleums are included, the range of values increases to 40 bar and 20 Sm^3/Sm^3.

Results from each of the North American petroleums are different to each other and different to those generated from the North Sea petroleums (Table 6). The North American black oil gives saturation pressures which are only half those derived from the North Sea petroleums, and much lower GOR and %CH_4 values.

The main implication of the results in Table 6 is that very consistent physical properties of included petroleums are derived if the initial choice of model petroleum is genetically related to the included petroleum. It is not essential that the starting petroleum is compositionally similar to that of the included petroleum, although the use of extreme compositions, such as recombined gas condensates, will increase the uncertainty of the calculated physical properties. The use of petroleums generated from source facies distinct to that of included petroleum should be avoided.

5.4. Overall precision: data from coeval inclusions

We now establish the overall precision with which the physical properties of included petroleums may be calculated by studying petroleum inclusions which appear to have formed coevally. We have used the four secondary inclusions described in the previous section.

The results of these analyses are given in Table 6. The homogenisation temperatures of these inclusions ranged from 68.3 to 69.9°C and the volume % vapour measured with the CLSM varied from 5.1 to 5.7. As before, the same gas titration strategy (Method 4) was used in all tests and the key results are summarized below:

1. Using a single North Sea petroleum as the starting fluid generates a range for the four inclusions of 20 bar (12% of the absolute value) in the saturation pressure and of 17 Sm^3/Sm^3 (19%) in the GOR.
2. The four North Sea petroleums give very similar results for each inclusion and thus the same range for the four inclusions as that from a single North Sea petroleum.
3. The two recombined North Sea petroleums give lower values of GOR and saturation pressure compared to those derived from the North Sea petroleums. Combining the results of the natural and recombined fluids, the total range for the four inclusions is 60 bars saturation pressure (35% of the absolute value) and 40 Sm^3/Sm^3 (45%) in the GOR.
4. Using the North American volatile oil as the starting fluid gives saturation pressures and GORs which are within the range of those generated from the recombined North Sea petroleums.
5. Use of the North American black oil as the starting fluid yields physical properties for the included petroleums which are consistent between the inclusions but which are very different to those generated from any of the other fluids.
6. Use of any fluid as the starting composition yields physical property data which are similar for each of the four inclusions; in these cases, a range of saturation pressures of around 20 bar (12% of the absolute value) and a range of GORs of around 20 Sm^3/Sm^3 (23%). However, the calculated physical properties differ depending on the compositional makeup of the starting fluid.

5.5. Pressure correction

The technique outlined here calculates, amongst other properties, the saturation pressure and isochore of the petroleum. It thus determines the minimum pressure of

Table 6
Calculated physical properties of petroleums trapped in four coeval, secondary petroleum inclusions in quartz from a North Sea reservoir. The compositions of the seven model petroleums used to calculate the properties are given in Table 5

	N. Sea 1	N. Sea 2	N. Sea 3	N. Sea 4	N. Sea 5	N. Sea 6	N. Am. 1	N. Am. 2
Inclusion 1								
Thom (C)	68.9	68.9	68.9	68.9	68.9	68.9	68.9	68.9
% Liquid	94.3	94.3	94.3	94.3	94.3	94.3	94.3	94.3
% Vapour	5.7	5.7	5.7	5.7	5.7	5.7	5.7	5.7
GOR STP (Sm^3/Sm^3)	101	102	102	95	80	96	84	88
CH_4 (mole %)	39.8	40.4	38.5	38.1	39.1	38.1	23.3	33.3
Sat P (bar)	186	177	176	171	151	167	90	140
Molar vol (cm^3/mol)	163.9	167.6	170.5	160.8	173.2	169.8	162.3	166.3
Ave dens. (g/cm^3)	0.747	0.733	0.728	0.754	0.723	0.734	0.731	0.735
Viscosity (cP)	0.472	0.461	0.466	0.460	0.465	0.467	0.486	0.441
Surface tension (mN/m)	0.17	0.14	0.097	0.234	0.109	0.078	0.262	0.136
Inclusion 2								
Thom (C)	69	69	69	69	69	69	69	69
% Liquid	94.9	94.9	94.9	94.9	94.9	94.9	94.9	94.9
% Vapour	5.1	5.1	5.1	5.1	5.1	5.1	5.1	5.1
GOR STP (Sm^3/Sm^3)	84	84	84	79	63	78	65	70
CH_4 (mole %)	37.0	36.0	35.7	35.1	36.2	34.8	20.7	29.8
Sat P (bar)	167	158	156	152	128	146	78	120
Molar vol (cm^3/mol)	175.9	180.5	183.9	172.4	187.3	183.2	175.4	179.6
Ave dens. (g/cm^3)	0.762	0.748	0.743	0.769	0.738	0.749	0.751	0.752
Viscosity (cP)	0.553	0.542	0.545	0.531	0.533	0.541	0.476	0.514
Surface tension (mN/m)	0.119	0.097	0.067	0.166	0.075	0.054	0.26	0.092
Inclusion 3								
Thom (C)	69.9	69.9	69.9	69.9	69.9	69.9	69.9	69.9
% Liquid	94.8	94.8	94.8	94.8	94.8	94.8	94.8	94.8
% Vapour	5.2	5.2	5.2	5.2	5.2	5.2	5.2	5.2
GOR STP (Sm^3/Sm^3)	85	85	85	79	65	79	66	71
CH_4 (mole %)	37.3	36.4	35.9	35.2	36.4	35.1	20.9	30.1
Sat P (bar)	169	160	158	153	131	148	79	122
Molar vol (cm^3/mol)	175.3	179.9	183.3	172.3	186.7	182.5	174.8	179.0
Ave dens. (g/cm^3)	0.761	0.747	0.741	0.768	0.736	0.747	0.749	0.750
Viscosity (cP)	0.546	0.534	0.538	0.532	0.527	0.535	0.470	0.507
Surface tension (mN/m)	0.121	0.098	0.068	0.167	0.076	0.055	0.265	0.093
Inclusion 4								
Thom (C)	68.3	68.3	68.3	68.3	68.3	68.3	68.3	68.3
% Liquid	94.8	94.8	94.8	94.8	94.8	94.8	94.8	94.8
% Vapour	5.2	5.2	5.2	5.2	5.2	5.2	5.2	5.2
GOR STP (Sm^3/Sm^3)	88	88	87	83	67	82	69	73
CH_4 (mole %)	37.6	36.9	36.3	36.0	36.4	35.5	21.3	30.5
Sat P (bar)	170	162	160	157	132	150	81	124
Molar vol (cm^3/mol)	173.7	177.5	180.8	168.8	183.9	180.0	172.2	176.4
Ave dens. (g/cm^3)	0.759	0.745	0.740	0.765	0.735	0.746	0.747	0.748
Viscosity (cP)	0.539	0.527	0.531	0.518	0.520	0.528	0.462	0.500
Surface tension (mN/m)	0.13	0.106	0.073	0.185	0.083	0.059	0.288	0.101

trapping, just as the homogenisation temperature gives the minimum temperature of trapping. The true trapping pressure lies somewhere along the petroleum's isochore, in the single phase region of P–T space. The difference between the minimum and true trapping temperature and pressure (the 'pressure correction') depends on how close the included petroleum was to being saturated with gas when trapped. Petroleums may be highly undersaturated and the pressure correction can be large (30°C and 100 bar are probably not uncommon). Determination of the true trapping pressure therefore requires a coexisting aqueous inclusion. As described by Roedder & Bodnar (1980), this allows one to construct a diagram comprising the phase envelopes and isochores of the aqueous and petroleum fluids. The true trapping pressure and temperature lies at the intersection of the two isochores. The isochores of methane-rich aqueous fluids are very steep and it is common to assume that the true trapping temperature of aqueous inclusions in petroleum systems are within a degree or two of the homogenisation temperature. In this case the key is to find coevally formed petroleum and aqueous inclusions.

6. Case studies

In this section we present two examples of the type of data which can be produced from the confocal technique. As our aim in this paper is to illustrate the potential of the confocal approach, only general geological background is given.

6.1. Ula Field, North Sea

The Ula Field in the North Sea contains diagenetic cements with abundant petroleum bearing fluid inclusions (Karlsen et al., 1993). The GOR of presently reservoired petroleum varies between 87 and 120 Sm^3/Sm^3 (Larter et al., 1990) and the maturity of petroleum within fluid inclusions hosted in different diagenetic phases varies considerably (Karlsen et al., 1993). These data suggest a relatively complex filling history for the reservoir, with the possibility that petroleum with distinct GORs entered the reservoir at different times in its history.

The homogenisation temperature of a primary, 3 μm petroleum bearing fluid inclusion hosted at the dust rim between a detrital quartz core and overgrowth was 90.1°C, with a liquid:vapour ratio of 80:20% (4:1) measured using normal white light. Using CLSM, the measured liquid:vapour ratio is 93.5:6.5% (14:1). The CLSM reveals that this fluid inclusion, like many others we have studied, has a highly irregular geometry. The petroleum initially chosen to model the included petroleum had a GOR of 65 Sm^3/Sm^3 at STP, a methane content of 26.5 mole % and a C_{20+} content of 18.4 mole % with a mean molecular weight of 421.0. At the homogenisation temperature of 90.1°C, the calculated saturation pressure of the included petroleum is 121 bar, compared to 160 bar for the current fluid in the Ula Formation reservoir (Larter et al., 1990). These are the minimum trapping pressure and temperature and we would require data from a coeval aqueous inclusion to determine the true trapping temperature and pressure, which lie somewhere along the isochore of the final petroleum (slope of 4.48 bar/°C).The calculated GOR of the included petroleum is 63 Sm^3/Sm^3, lower than that presently within the same reservoir unit (120 Sm^3/Sm^3). The methane content (25.6 mole %) is slightly lower than that presently in the Ula formation reservoir (29 mole %) but higher than that of the petroleum in the underlying Skagerrak reservoir (21 mole %; Larter et al., 1990). These data support the previously published reservoir filling model involving a relatively recent influx of more mature and gas-rich petroleum into the Ula Formation reservoir (Larter et al., 1990).

6.2. Central North Sea

These data come from a reservoir in the high pressure and high temperature part of the Central North Sea. The current (maximum) reservoir temperature and pressure are 162°C and 847 bar at approximately 4.3 km depth. The fluid in the well from which the fluid inclusions were studied is a volatile oil with a GOR of around 3000 scf/bbl (534 Sm^3/Sm^3).

Clusters of inclusions with similar homogenisation temperatures were identified in samples from two horizons. Since we are interested in the evolution of fluid composition, both primary and secondary inclusions were analysed. Microthermometric and CLSM analyses were performed on 19 inclusions. The physical properties of the included petroleums were detemined using the reservoir oil as the model petroleum and a titrant gas derived by flashing the same oil at atmospheric pressure and a temperature 50°C higher than the homogenisation temperature of the inclusion (Method 4 above).

All the inclusions homogenised into a single phase liquid at temperatures between 78–110°C (Fig. 4). CLSM analysis showed that the vapour contents of the inclusions ranged from 5–25%. Calculated GORs vary widely from 400–2500 scf/bbl (71–445 Sm^3/Sm^3), generally increasing over a 15°C rise in homogenisation temperature (Fig. 4). Although the inclusions record the presence of a wide range of petroleum compositions during the filling history of the reservoir, the precise temperature (and thus time if an appropriate time-temperature history is available) at which individual petroleums were present in the reservoir cannot be assessed without data from coeval aqueous inclusions to constrain the pressure correction.

The plot of the included petroleums'–saturation pressures (minimum trapping pressure) against homogenisation temperatures (minimum trapping temperatures) in Fig. 4 shows a general trend to higher pressures at higher temperatures. The range of saturation pressures is between 200 and 400 bar, much lower than the current reservoir pressure (847 bar) and within 100 bar of the probable hydrostatic pressure at the time. Since these oils are undersaturated, the true trapping pressures will be higher than the saturation pressures and will lie somewhere along the petroleums' isochores. Isochores and phase envelopes of currently reservoired petroleum and of two included petroleums are shown in Fig. 5. The slopes of the isochores vary between about 3.0 and 3.9 bar/°C. Projection of the isochores on Fig. 4 gives pressures no higher than 550 bar at present reservoir temperature, suggesting that the rate at which pressure has increased in this reservoir has been very rapid since the inclusions were trapped. Suggestions of a rapid rise in fluid pressure is qualitatively consistent with the rapid burial that this part of the Central North Sea has undergone in the last few million years (Stewart, 1986).

7. Conclusions

In this paper we have introduced a methodology for estimating the phase envelope, isochore and physical

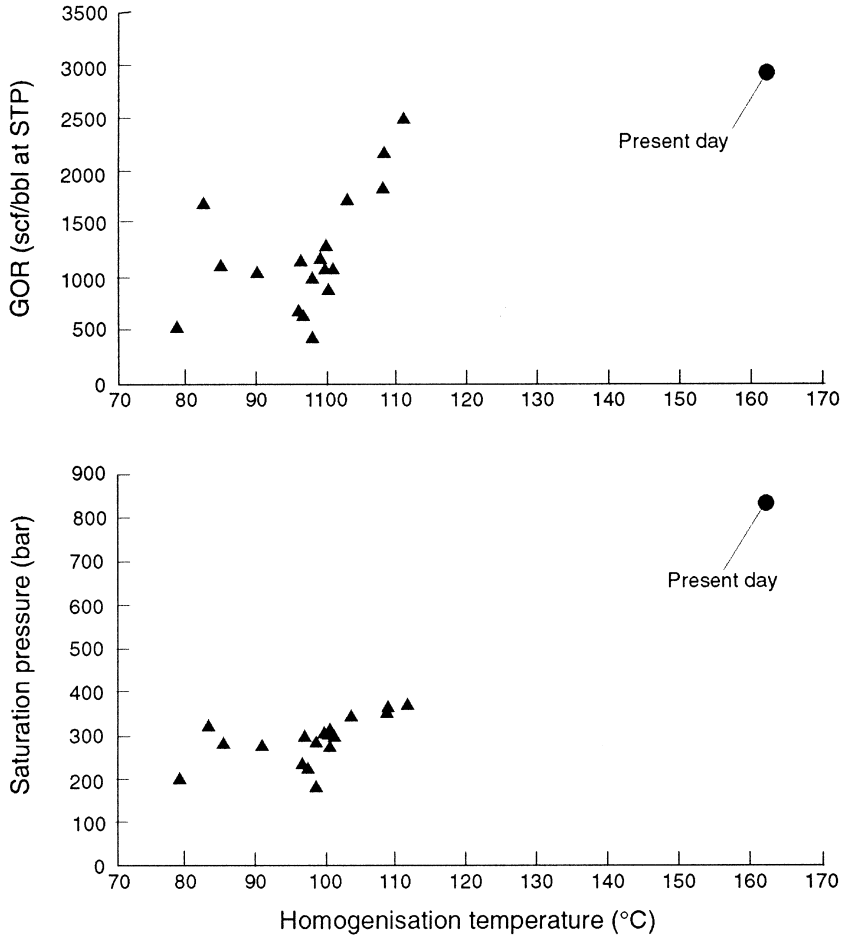

Fig. 4. Calculated Gas–Oil Ratio ($GOR = C_{1-5}/C_{6+}$) and saturation pressure vs homogenisation temperature for fluid inclusions in a Central North Sea well. Present day conditions are also shown.

properties of petroleum hosted within single fluid inclusions. Based on the analysis of coeval petroleum inclusions, we believe that the method calculates the saturation pressure, GOR, viscosity, molar volume, density and surface tension of included petroleum with a *precision* of a few percent. Data generated from a study of a Central North Sea reservoir are consistent, geologically realistic and provide, for the first time, an estimate of the way in which the fluid pressure and petroleum composition of a reservoir evolved through time. Confirmation of the *accuracy* of the method awaits tests using inclusions grown in the laboratory under carefully controlled PVTX conditions. However, it is likely that the physical properties of included petroleums are most accurately modelled by fluids which are genetically related to them.

If validated, this technique will allow semi-routine palaeobarometry in situations where coeval aqueous and petroleum inclusions exist (Roedder & Bodnar, 1980). For the first time, these data will constrain the outputs of basin simulators, which calculate fluid pressures through time.

Acknowledgements

This work has been funded by the EU Thermie program and by the Geosciences Project on Overpressure (GeoPOP) consortium of companies: Agip, Amerada Hess, Amoco, ARCO, Conoco, Elf Enterprise, Enterprise UK, Mobil, Norsk Hydro, Phillips Petroleum Company Limited, Statoil and Total. Ashley Bigge generously provided the data in Fig. 3 and Table 1. The Central North Sea data were generated using funds from an EU Thermie award to BP, Elf and IFP. Barbara Brown and Christine Jeans produced the artwork and graphics whilst Don Hall, Dick Swarbrick, Mark Osborne, Gareth Yardley, Rebecca Lloyd and Mark Parfitt shared useful ideas. Finally, many thanks to Norman Oxtoby and an anony-

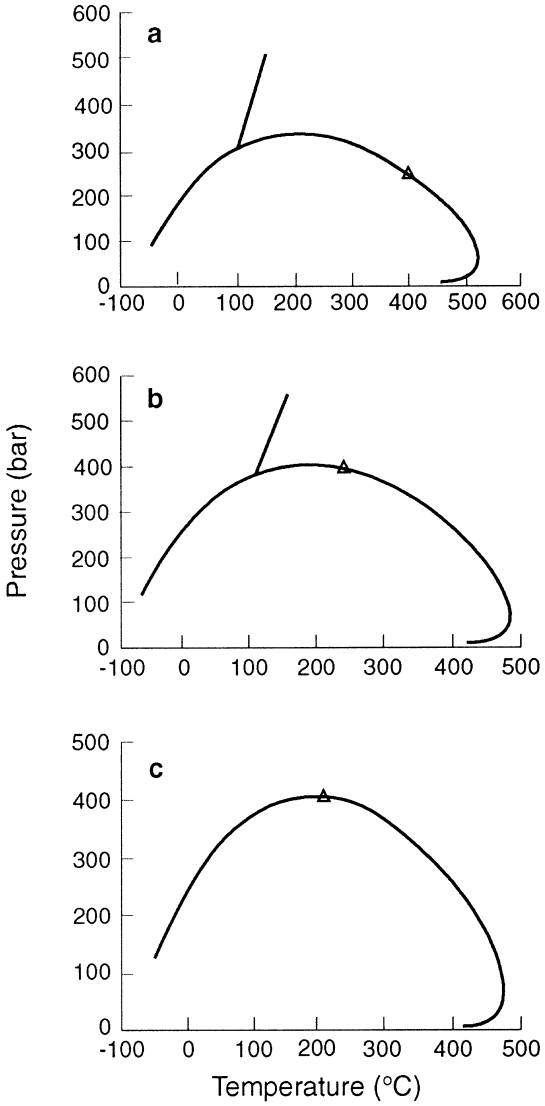

Fig. 5. Calculated P–T phase diagrams and isochores for petroleums in two fluid inclusions (a) $T_{hom} = 100.8°C$; (b) $T_{hom} = 110.9°C$) from a Central North Sea field, plus (c) the P–T phase diagram for the current reservoir fluid. Critical points denoted by triangles on the phase envelopes.

mous reviewer for their efforts in improving the original manuscript.

References

Bigge, M. A., Petch, G. S., Macleod, G., Larter, S. R., & Aplin, A. C. (1995). Quantitative geochemical analysis of petroleum fluid inclusions: Problems and developments. In J.O. Grimalt, C. Dorronsoro (Eds.), *Proceedings 17th International Meeting on Organic Geochemistry*(pp. 757–759). European Association of Organic Geochemists: San Sebastian.

Bodnar, R. J. (1990). Petroleum migration in the Miocene Monterey Formation, California, USA: constraints from fluid inclusion studies. *Mineralogical Magazine*, *54*, 295–304.

Burruss, R. C. (1987) Crushing-cell, capillary column gas chromatography of petroleum fluid inclusions: Method and application to petroleum source rocks, reservoirs and low temperature hydrothermal ores (Abstract). In: *PACROFI, Pan American Conference on Research on Fluid Inclusions*, Program and Abstracts, Socorro, NM, (unpaginated)

Burruss, R. C. (1992) Phase behaviour in petroleum–water (brine) systems applied to fluid inclusion studies (Abstract). In: *PACROFI IV, Pan American Conference on Research on Fluid Inclusions*, Program and Abstracts, Lake Arrowhead, CA, 4, 116–118

Danesh, A., Xu, D. H., & Todd, A. C. (1991). Comparative study of cubic equations of state for predicting phase behaviour and volumetric properties of injection gas-reservoir oil systems. *Fluid Phase Equilibria*, *63*, 259–278.

Earnshaw, J. P., Hogg, A. J. C., Oxtoby, N. H., & Cawley, S. J. (1993). Petrographic and fluid inclusion evidence for the timing of diagenesis and petroleum entrapment in the Papuan Basin. In G.J. Carman (Ed.), *Proceedings of the Second PNG Petroleum Convention*(pp. 459–475). Port Moresby.

Goldstein, R. H., & Reynolds, T. J. (1994). Systematics of fluid inclusions in diagenetic minerals. *Society for Sedimentary Geology Short Course*, *31*, 199.

Guilhaumou, N., Szydlowskii, N., & Pradier, B. (1990). Characterization of hydrocarbon fluid inclusions by infra-red and fluorescence microscopy. *Mineralogical Magazine*, *54*, 311–324.

Isaksen, G., Pottorf, R. J., & Jenssen, A. I. (1998). Correlation of fluid inclusions and reservoired oils to infer trap fill history in the South Viking Graben, North Sea. *Petroleum Geoscience*, *4*, 41–55.

Jensenius, J., & Burruss, R. C. (1990). Hydrocarbon-water interactions during brine migration: Evidence from hydrocarbon inclusions in calcite cements from Danish North Sea oil fields. *Geochimica et Cosmochimica Acta*, *54*, 705–714.

Jones, D. M., Macleod, G., Larter, S. R., Hall, D. L., Aplin, A. C., & Chen, M. (1996). Characterisation of the molecular composition of included petroleum. In P.E. Brown, S.G. Hagemann (Eds.), *Biennial Pan-American Conference on Research on Fluid Inclusions (PACROFI VI)*(pp. 64–65). Wisconsin, USA: Madison.

Karlsen, D., Nedkvitne, T., Larter, S. R., & Bjørlykke, K. (1993). Hydrocarbon composition of authigenic inclusions: Applications to elucidation of petroleum reservoir filling history. *Geochimica et Cosmochimica Acta*, *57*, 3641–3659.

Kihle, J. (1996). Adaptation of fluorescence excitation-emission microspectroscopy for characterization of single hydrocarbon fluid inclusions. *Organic Geochemistry*, *23*, 1029–1042.

Larese, R. E., & Hall, D. L. (1996). Studying petroleum migration with fluid inclusions: Results from hydrothermal burial simulation experiments. In P.E. Brown, S.G. Hagemann (Eds.), *Biennial Pan-American Conference on Research on Fluid Inclusions (PACROFI VI)*(pp. 74–75). Wisconsin, USA: Madison.

Larter, S. R., Bjørlykke, K. O., Karlsen, D. A., Nedkvitne, T., Eglinton, T., Johansen, P. E., Leythauser, D., Mason, P. C., Mitchell, A. W., & Newcombe, G. A. (1990). Determination of petroleum accumulation histories: examples from the Ula Field, Central Graben, Norwegian N. sea. In A. Buller (Ed.), *North Sea Oil and Gas Reservoirs–II*(pp. 319–330). NPF Trondheim.

Lisk, M., George, S. C., Summons, R. E., Quezada, R. A., & O'Brien, G. W. (1996). Mapping hydrocarbon charge histories: detailed characterisation of the South Pepper Oil Field, Carnarvon Basin. *APPEA Journal*, *36*, 445–463.

Macleod, G., Larter, S. R., Aplin, A. C., & Petch, G. S. (1994). Improved analysis of petroleum fluid inclusions: Application to reservoir studies. *Abstracts of The American Chemical Society*, *207*, 132.

Macleod G., Larter S.R., Aplin A.C., Bigge M.A. 1995 The application of petroleum bearing fluid inclusions to tracking petroleum evolution. In: *European Association of Geoscientists and Engineers, 57th Conference and Technical Exhibition*, Paper F033, Glasgow

Macleod, G., Larter, S. R., Aplin, A. C., Pedersen, K. S., & Booth, T. A. (1996). Determination of the effective composition of single

petroleum inclusions using Confocal Scanning Laser Microscopy and PVT simulation. In P.E. Brown, S.G. Hagemann (Eds.), *Biennial Pan-American Conference on Research on Fluid Inclusions (PACROFI VI)* (pp. 81–82). Wisconsin, USA: Madison.

McLimans, R. K. (1987). The application of fluid inclusions to migration of oil and diagenesis in petroleum reservoirs. *Applied Geochemistry*, *2*, 585–603.

McLimans, R. K., & Horsfield, B. (1984). Geothermometry and geochemistry of aqueous and oil-bearing fluid inclusions from Fateh Field, Dubai. *Organic Geochemistry*, *6*, 733–740.

Narr, W., & Burruss, R. (1984). Origin of reservoir fractures in Little Knife Field, North Dakota. *American Association Petroleum Geologists Bulletin*, *68*, 1087–1100.

Pedersen K.S., Fredenslund Aa, Thomassen P. (1989) Properties of oils and natural gases. *Contributions in Petroleum Geology and Engineering 5*, 252. Gulf Publishing Company

Pironon, J., & Barrés, O. (1990). Semi-quantitative FT-IR microanalysis limits: Evidence from synthetic hydrocarbon fluid inclusions in sylvite. *Geochimica et Cosmochimica Acta*, *54*, 509–518.

Pironon, J., & Barrés, O. (1992). Influence of brine-hydrocarbon reactions on FT-IR microspectroscopic analysis of intracrystalline liquid inclusions. *Geochimica et Cosmochimica Acta*, *56*, 169–174.

Roedder E. 1984 Fluid Inclusions. *Reviews in Mineralogy 12*, 644. American Mineralogical Society.

Roedder, E., & Bodnar, R. J. (1980). Geologic pressure determinations from fluid inclusion studies. *Ann. Rev. Earth. Planet. Sci.*, *8*, 263–301.

Sheppard, C. J. R., & Shotton, D. M.(1997). . In *Confocal Laser Scanning Microscopy*. Oxford, UK: BIOS Scientific Publishers.

Stewart, D. J. (1986). Diagenesis of the shallow marine Fulmar Formation in the Central North Sea. *Clay Minerals*, *21*, 537–564.

Swarbrick, R. E. (1994). Reservoir diagenesis and hydrocarbon migration under hydrostatic palaeopressure conditions. *Clay Minerals*, *29*, 463–473.